JOURNAL OF GEOPHYSICAL RESEARCH, VOL. 114, D04305, doi:10.1029/2007JD009264, 2009

Comparison of adjoint and analytical Bayesian inversion methods for constraining Asian sources of carbon monoxide using satellite (MOPITT) measurements of CO columns

Monika Kopacz,[1] Daniel J. Jacob,[1] Daven K. Henze,[2] Colette L. Heald,[3] David G. Streets,[4] and Qiang Zhang[4]

Received 9 August 2007; revised 30 September 2008; accepted 19 December 2008; published 19 February 2009.

[1] We apply the adjoint of an atmospheric chemical transport model (GEOS-Chem CTM) to constrain Asian sources of carbon monoxide (CO) with 2° × 2.5° spatial resolution using Measurement of Pollution in the Troposphere (MOPITT) satellite observations of CO columns in February–April 2001. Results are compared to the more common analytical method for solving the same Bayesian inverse problem and applied to the same data set. The analytical method is more exact but because of computational limitations it can only constrain emissions over coarse regions. We find that the correction factors to the a priori CO emission inventory from the adjoint inversion are generally consistent with those of the analytical inversion when averaged over the large regions of the latter. The adjoint solution reveals fine-scale variability (cities, political boundaries) that the analytical inversion cannot resolve, for example, in the Indian subcontinent or between Korea and Japan, and some of that variability is of opposite sign which points to large aggregation errors in the analytical solution. Upward correction factors to Chinese emissions from the prior inventory are largest in central and eastern China, consistent with a recent bottom-up revision of that inventory, although the revised inventory also sees the need for upward corrections in southern China where the adjoint and analytical inversions call for downward correction. Correction factors for biomass burning emissions derived from the adjoint and analytical inversions are consistent with a recent bottom-up inventory on the basis of MODIS satellite fire data.

Citation: Kopacz, M., D. J. Jacob, D. K. Henze, C. L. Heald, D. G. Streets, and Q. Zhang (2009), Comparison of adjoint and analytical Bayesian inversion methods for constraining Asian sources of carbon monoxide using satellite (MOPITT) measurements of CO columns, *J. Geophys. Res.*, *114*, D04305, doi:10.1029/2007JD009264.

1. Introduction

[2] Inverse modeling is a standard tool for combining observations of atmospheric composition with knowledge of atmospheric processes (transport, chemistry) to derive quantitative constraints on emissions to the atmosphere. A chemical transport model (CTM), known as the forward model for the inversion, solves the continuity equation to predict concentrations as a function of emissions. The inverse model then optimizes the emission estimates by fitting the CTM to the observed concentrations, subject to error weighting and a priori information on the emissions. We compare here analytical and adjoint methods for the inverse problem as applied to optimization of Asian emissions of carbon monoxide (CO) using Measurement of Pollution in the Troposphere (MOPITT) satellite observations of CO atmospheric columns [*Deeter et al.*, 2002]. We demonstrate the ability of the adjoint approach to constrain emissions with high resolution when using a large satellite data set, revealing aggregation errors in the analytical method.

[3] Consider the general problem of estimating a set of emissions (assembled in a state vector $\mathbf{x}$), given a set of observed atmospheric concentrations (observation vector $\mathbf{y}$) and a CTM forward model $\mathbf{y} = \mathbf{F}(\mathbf{x})$. One can define an optimal value of $\mathbf{x}$ as that which minimizes an error-weighted least squares (chi-square) scalar cost function $J(\mathbf{x})$, derived from Bayes' theorem with the assumption of Gaussian errors [*Rodgers*, 2000]. The cost function describes the error-weighted mismatch between the observed concentrations, $\mathbf{y}$, and those simulated with the forward model, $\mathbf{F}(\mathbf{x})$, as well as the error-weighted mismatch between the true state and the a priori estimate $\mathbf{x_a}$. The solution for $\min(J(\mathbf{x}))$ with respect to $\mathbf{x}$ such that $\nabla_{\mathbf{x}} J(\mathbf{x}) = \mathbf{0}$ defines the Maximum A Posteriori (MAP) solution of the inverse problem [*Rodgers*, 2000].

[4] Most of the inverse modeling literature for atmospheric composition has used an analytical solution for $\nabla_{\mathbf{x}} J(\mathbf{x}) = \mathbf{0}$,

[1]Division of Engineering and Applied Science, Harvard University, Cambridge, Massachusetts, USA.
[2]Department of Mechanical Engineering, University of Colorado, Boulder, Colorado, USA.
[3]Department of Atmospheric Science, Colorado State University, Fort Collins, Colorado, USA.
[4]Decision and Information Sciences Division, Argonne National Laboratory, Argonne, Illinois, USA.

0148-0227/09/2007JD009264$09.00

and we refer to this here as the "analytical method." It has been applied extensively for example for inverse modeling of CO_2 surface fluxes and CO emissions using observations from surface sites [*Bousquet et al.*, 1999; *Bergamaschi et al.*, 2000; *Kasibhatla et al.*, 2002; *Pétron et al.*, 2002] and aircraft [*Palmer et al.*, 2003; *Palmer et al.*, 2006]. Computing this analytical solution involves construction of the CTM Jacobian matrix ($\mathbf{K} = \partial\mathbf{y}/\partial\mathbf{x}$) and subsequent multiplication and inversion of matrices with dimensions of dim($\mathbf{x}$) and dim($\mathbf{y}$). This limits the practical size of $\mathbf{x}$, i.e., the number of emission regions that can be optimized (limitations in the size of $\mathbf{y}$ can be overcome by partitioning the observations into independent packets assimilated by the inversion, i.e., "sequential updating" [*Rodgers*, 2000]). However, a large state vector $\mathbf{x}$ is desirable in applying the inverse method to satellite observations, where one would like to exploit the richness of the data to constrain emissions with high spatial and temporal resolution, limited only by the resolution of the CTM used as the forward model.

[5] An alternative to the analytical method is to seek a numerical solution to $\nabla_{\mathbf{x}} J(\mathbf{x}) = \mathbf{0}$ by using the CTM adjoint to efficiently compute $\nabla_{\mathbf{x}} J(\mathbf{x})$ from successive estimates of $\mathbf{x}$ starting with the a priori, and applying an iterative optimization algorithm to converge to the solution. We refer to this here as the "adjoint method." Pioneering studies applying the adjoint method to optimize emissions include the work of *Elbern et al.* [1997], *Eibern and Schmidt* [1999], and *Kaminski et al.* [1999]. Recent studies have applied the method to constrain aerosol emissions [*Hakami et al.*, 2005; *Dubovik et al.*, 2008], global CO and NO_x emissions using surface measurements of CO from the NOAA/CMDL network and NO_2 columns from the GOME satellite instrument [*Müller and Stavrakou*, 2005], global CO emissions using MOPITT columns [*Stavrakou and Müller*, 2006], and East Asian CO sources using measurements from ground stations [*Yumimoto and Uno*, 2006].

[6] Inversion of CO sources is an attractive application of the adjoint method because of the availability of dense and high-quality satellite observations. The MOPITT instrument is a nadir viewing pressure modulator radiometer that measures broadband infrared radiation in thermal emission, from which CO column and profile concentrations are retrieved. It was launched onboard NASA's EOS Terra in 1999 in a sun-synchronous polar orbit [*Deeter et al.*, 2002], provides measurements with 1–2 pieces of information in the vertical and global coverage every 3 days. CO is emitted by incomplete combustion and is also produced in the atmosphere by oxidation of volatile organic compounds (VOCs). Its sink is oxidation by OH with a lifetime of about two months. Several recent inverse studies have used MOPITT CO data to constrain CO sources [*Arellano et al.*, 2004; *Heald et al.*, 2004; *Pétron et al.*, 2004; *Arellano et al.*, 2006; *Stavrakou and Müller*, 2006; *Arellano et al.*, 2007]. All, except *Stavrakou and Müller* [2006], used the analytical method. *Arellano et al.* [2006] constrained a state vector of emissions including over 100 elements, much larger than previous studies, but still not commensurate to the density of data provided by MOPITT.

[7] *Stavrakou and Müller* [2006] applied an adjoint method to 2000–2001 MOPITT CO columns to constrain global CO sources, and compared "large region" and "grid-based" approaches to the inversion. This corresponded to CO source inversion at low (18 regions) versus high ($5^\circ \times 5^\circ$) resolution, in both cases using an adjoint of the IMAGES CTM driven by monthly mean wind fields. They found that the grid-based inversion yielded better agreement with the observed CO columns and allowed for greater exploitation of the data. Here we also constrain CO sources at the native resolution of our CTM ($2^\circ \times 2.5^\circ$), but rather than assess the impact of the resolution alone, we compare the adjoint to the analytical inversion method. Adjoint and analytical methods yield theoretically the same MAP solution but practically we may expect differences from the numerical approximation involved in the adjoint method. In addition, the analytical method provides exact covariance information on the solution which the adjoint method does not.

[8] We focus our analysis on Asian CO sources using MOPITT observations for the March–April 2001 period of the NASA/TRACE-P aircraft mission over the NW Pacific. This mission focused on characterizing the chemical outflow from the Asian continent and provided validation data for MOPITT [*Jacob et al.*, 2003]. *Palmer et al.* [2003] and *Wang et al.* [2004] previously used the TRACE-P aircraft observations to invert for Asian CO sources, using as a priori a detailed Asian emissions inventory for 2000 [*Streets et al.*, 2003]. *Heald et al.* [2004] compared the information content from the TRACE-P aircraft and MOPITT satellite observations as constraints on Asian CO sources and concluded that the satellite observations were far richer. All these studies used the analytical method for the inversion. Additional studies for the TRACE-P period used simpler methods to constrain Asian CO sources from the aircraft and MOPITT observations [*Carmichael et al.*, 2003; *Allen et al.*, 2004], all with consistent results. March–April 2001 thus represents a well-studied period for Asian CO sources, and the study of *Heald et al.* [2004] is of particular value to us as a reference for the analytical solution to the inverse problem.

2. Analytical Versus Adjoint Solutions to the Inverse Problem

[9] We address the inverse problem of determining emissions $\mathbf{x}$ given observed atmospheric concentrations $\mathbf{y}$ and a CTM forward model:

$$\mathbf{y} = \mathbf{F}(\mathbf{x}) + \boldsymbol{\varepsilon} \tag{1}$$

where $\boldsymbol{\varepsilon}$ is the "observation error" including contributions from the measurements and from imperfection in the forward model (e.g., transport error). We apply an a priori constraint $\mathbf{x_a}$ on the emissions subject to error $\boldsymbol{\varepsilon_a}$. Application of Bayes' theorem with assumption of Gaussian errors leads to a MAP solution for $\mathbf{x}$ given $\mathbf{y}$ as the minimum of the cost function $J(\mathbf{x})$ [*Rodgers*, 2000]:

$$J(\mathbf{x}) = (\mathbf{F}(\mathbf{x}) - \mathbf{y})^{\mathrm{T}} \mathbf{S}_{\Sigma}^{-1} (\mathbf{F}(\mathbf{x}) - \mathbf{y}) + \gamma (\mathbf{x} - \mathbf{x_a})^{\mathrm{T}} \mathbf{S}_{\mathbf{a}}^{-1} (\mathbf{x} - \mathbf{x_a}) \tag{2}$$

Here $\mathbf{S}_{\Sigma}$ and $\mathbf{S_a}$ are the observational and a priori error covariance matrices representing the error statistics of $\boldsymbol{\varepsilon}$ and $\boldsymbol{\varepsilon_a}$, respectively. The regularization parameter γ controls the relative constraints applied by the observational and a priori parts of the cost function [*Hakami et al.*, 2005; *Müller and Stavrakou*, 2005; *Yumimoto and Uno*, 2006; *Henze et al.*, 2007]. Bayes' theorem would have $\gamma = 1$, but this assumes that $\mathbf{S}_{\Sigma}$ and $\mathbf{S_a}$ are adequately characterized, which is difficult

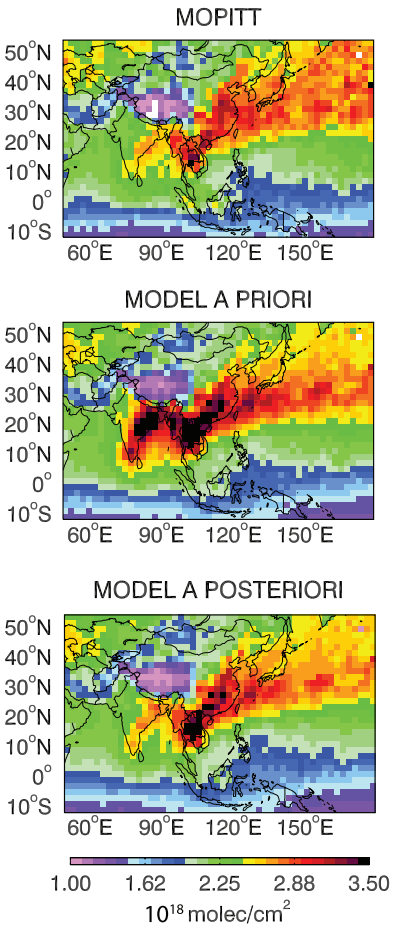

Figure 1. Mean atmospheric CO columns over eastern Asia and downwind for the TRACE-P period (21 February to 10 April 2001). (top) MOPITT satellite observations and GEOS-Chem model values using (middle) a priori and (bottom) a posteriori CO sources (Table 1). The GEOS-Chem values are smoothed with the local MOPITT averaging kernels.

to achieve in practice. To our knowledge, all inverse studies in the literature employing the analytical method have used $\gamma = 1$, and since in those studies $\dim(\mathbf{x}) \ll \dim(\mathbf{y})$ there is little influence of the a priori on the solution. Studies using the adjoint method have determined γ by analyzing its influence on the minimum of $J(\mathbf{x})$ [*Hakami et al.*, 2005; *Yumimoto and Uno*, 2006; *Henze et al.*, 2007].

[10] Minimization of $J(\mathbf{x})$ is the objective of both the analytical and adjoint methods; this corresponds to solving

$$\nabla_{\mathbf{x}} J(\mathbf{x}) = 2(\nabla_{\mathbf{x}}\mathbf{F})^{\mathrm{T}}\mathbf{S}_{\Sigma}^{-1}(\mathbf{F}(\mathbf{x}) - \mathbf{y}) + 2\gamma\mathbf{S}_{\mathbf{a}}^{-1}(\mathbf{x} - \mathbf{x}_{\mathbf{a}}) = \mathbf{0} \quad (3)$$

where $\nabla_{\mathbf{x}}\mathbf{F}$ is the Jacobian matrix of the forward model. Analytical solution to the Bayesian optimization problem as described by (3) yields the following expression for the MAP estimate $\hat{\mathbf{x}}$ and its error covariance matrix $\hat{\mathbf{S}}$ [*Rodgers*, 2000]:

$$\hat{\mathbf{x}} = \mathbf{x}_{\mathbf{a}} + ((\nabla_{\mathbf{x}}\mathbf{F})^{\mathrm{T}}\mathbf{S}_{\Sigma}^{-1}\nabla_{\mathbf{x}}\mathbf{F} + \gamma\mathbf{S}_{\mathbf{a}}^{-1})^{-1}(\nabla_{\mathbf{x}}\mathbf{F})^{\mathrm{T}}\mathbf{S}_{\Sigma}^{-1}(\mathbf{y} - \mathbf{F}(\mathbf{x}_{\mathbf{a}})) \quad (4)$$

$$\hat{\mathbf{S}}^{-1} = (\nabla_{\mathbf{x}}\mathbf{F})^{\mathrm{T}}\mathbf{S}_{\Sigma}^{-1}\nabla_{\mathbf{x}}\mathbf{F} + \gamma\mathbf{S}_{\mathbf{a}}^{-1} \quad (5)$$

[11] Computation of $\hat{\mathbf{x}}$ and $\hat{\mathbf{S}}$ from (4) and (5) requires explicit construction of the Jacobian matrix and multiplication and inversion of matrices of dimensions $\dim(\mathbf{x})$ and $\dim(\mathbf{y})$. Nonlinear forward models may require multiple iterations involving recalculation of the Jacobian at each iteration. Observation subsets are often sufficiently uncorrelated to be ingested sequentially in the inversion, thus reducing the $\mathbf{y}$ dimension of the matrices. However, this sequential updating [*Rodgers*, 2000] cannot be used to reduce the $\mathbf{x}$ dimension.

[12] The adjoint method overcomes this obstacle through numerical solution to $\nabla_{\mathbf{x}} J(\mathbf{x}) = \mathbf{0}$. The adjoint of the forward model, $(\nabla_{\mathbf{x}}\mathbf{F})^{\mathrm{T}}$, is the transpose of its Jacobian matrix. In equation (3), the adjoint is applied to the vector of error-weighted differences $2\mathbf{S}_{\Sigma}^{-1}(\mathbf{F}(\mathbf{x}) - \mathbf{y})$ between observations and the forward model. This enables rapid computation of $\nabla_{\mathbf{x}} J(\mathbf{x})$ and avoids explicit construction of the Jacobian $\nabla_{\mathbf{x}}\mathbf{F}$ [*Giering and Kaminski*, 1998; *Kaminski et al.*, 1999], which is a major disadvantage of the analytical method. Application of the adjoint method to observations over a forward time period $[t_o, t_f]$ begins by computing $(2\,\mathbf{S}_{\Sigma}^{-1}\,(\mathbf{F}(\mathbf{x_a}) - \mathbf{y}))$ from the observations at time t_f, using the a priori $\mathbf{x_a}$ as initial guess, and then applying the adjoint model back in time over $[t_f, t_o]$, assimilating additional observations along the way. Computational cost is mainly determined by the length of the simulation time period $[t_f, t_o]$, i.e., by the time horizon over which the state vector is to be optimized. The resulting value of $\nabla_{\mathbf{x}} J(\mathbf{x_a})$ is used with an optimization algorithm to obtain an improved estimate $\mathbf{x_1}$ of $\mathbf{x}$. We then rerun the forward model with this improved estimate to obtain concentrations $\mathbf{F}(\mathbf{x_1})$ for use in the subsequent adjoint run, calculate $\nabla_{\mathbf{x}} J(\mathbf{x_1})$, and iterate.

[13] Unlike the analytical method, the adjoint method does not systematically provide an a posteriori error covariance matrix $\hat{\mathbf{S}}$ by equation (5) since the Jacobian matrix is not calculated. Some optimization algorithms compute an approximation of the error covariance as part of the inversion [*Müller and Stavrakou*, 2005; *Baker et al.*, 2006]. We do not do so here, as the assumption of unbiased Gaussian observational errors produces Bayesian a posteriori errors that tend to be unrealistically small in any case. Past inverse modeling studies using the analytical method have pointed out that a better estimate of inverse model error can be obtained with an ensemble of calculations varying forward model parameters and error covariance specifications over their expected ranges of uncertainty [*Peylin et al.*, 2002; *Heald et al.*, 2004].

3. MOPITT Observations and a Priori Sources

[14] We use here the same MOPITT observations, forward model (GEOS-Chem CTM), a priori emissions, and error covariance matrices as in the inverse analysis of *Heald et al.* [2004]. The MOPITT data are daytime CO columns (1030 local time overpass) during the TRACE-P period (21 February to 10 April 2001) over the Asian domain (10°S–55°N, 50°E–180°E), and averaged over the 2° × 2.5° GEOS-Chem grid. This amounts to 21,569 observations (Figure 1). The "best case" MAP solution reported by *Heald et al.* [2004] used a slightly narrower latitudinal domain (0°–55°N) and included chi-square filtering of outliers, reducing the total number of observations to

Table 1. Optimization of CO Sources by Analytical and Adjoint Inverse Methods[a]

Source Region[b]	Source (Tg a^{-1})		A Posteriori to A Priori Source Ratio						
			Analytical Inversion						
	A Priori	*Streets et al.* [2006]	Best Estimate[c]	Ensemble Range[d]	Case 1[e]	Case 2[f]	Case 3[g]	Adjoint Inversion[h]	A Posteriori Source (Tg a^{-1})
Japan	7.7		2.67	(0.47–1.83)	1.69	1.87	1.88	1.11	8.5
Korea	6.3		2.67	(0.47–1.83)	1.69	1.87	1.88	0.94	5.9
N. China	9.6	10.1	0.32	(0.47–1.83)	0.87	0.72	0.76	1.13	10.8
C. China	52.9	66.9	1.48	(1.29–1.75)	1.56	1.59	1.83	1.34	70.9
W. China	33.0	34.1	2.12	(1.29–1.75)	2.30	2.13	2.38	1.10	36.3
S. China	25.0	41.8	0.87	(0.63–1.37)	0.42	0.50	0.31	0.94	23.5
SE Asia	69.2		0.61	(0.37–0.90)	0.64	0.68	0.63	0.78	54.0
Philippines	5.6		0.48	(0.48–1.11)	0.62	0.87	0.89	0.90	5.0
Indonesia	55.6		1.41	(1.01–1.14)	1.44	0.94	0.96	0.97	54.0
India	89.9		0.51	(1.01–1.14)	0.56	0.61	0.50	0.37	33.3
Europe	145		0.73	(1.01–1.14)	0.77	0.80	0.75	1.07	155
Rest of world	596		1.15	(1.01–1.14)	1.15	1.14	1.16	1.16	691
Methane and biogenic NMVOCs	1205		1.15	(1.01–1.14)	1.15	1.14	1.16	0.99	1193
Number of MOPITT observations			18,295	18,295	18,295	20,542	21,569	21,569	

[a]Sources for the TRACE-P period (February–April 2001), converted to equivalent Tg a^{-1} assuming no seasonal variation in fuel sources and a seasonal variation in biomass burning as described by *Duncan et al.* [2003]. The regional sources include direct emissions from fossil fuel, biofuel, and biomass burning, as well as chemical production from anthropogenic nonmethane volatile organic compounds (NMVOCs) coemitted with CO [*Duncan et al.*, 2006].

[b]Source regions are those of *Heald et al.* [2004] and follow the same numbering as in that paper. See Figure 3a for region boundaries. Japan and Korea were treated as one single source region in the *Heald et al.* [2004] analytical inversion, and so were the sources from oxidation of methane, biogenic NMVOCs, and emissions outside Eurasia (rest of world).

[c]Best case inverse solution from *Heald et al.* [2004] constraining an 11-element state vector using the analytical method. Relative to this best case from *Heald et al.* [2004], our adjoint solution presented here assumes uncorrelated observational error (no off-diagonal terms in the observational covariance matrix), uses an extended latitudinal domain (10°S–55°N versus 0°–55°N), and does not remove outliers in the MOPITT data (χ^2 filter). The effects of these successive modifications on the *Heald et al.* [2004] analytical inversion are shown in the Table as Cases 1–3.

[d]Range of source constraints obtained by *Heald et al.* [2004] in an ensemble of inversions with varying inversion parameters, corresponds to *Heald et al.* [2004, Figure 10].

[e]No observational error covariance.

[f]No observational error covariance, extended domain.

[g]No observational error covariance, extended domain, no χ^2 filter. These conditions reproduce exactly those used in the adjoint inversion (results in the next column).

[h]The adjoint inversion optimizes the CO source on the 2° × 2.5° grid of the GEOS-Chem CTM, and the solution is averaged here over the 11 regions of the analytical inversion for purpose of comparison. See Figure 5 for the fine structure of the adjoint solution.

18,295 (Table 1). For the purposes of our comparison we repeated the *Heald et al.* [2004] analytical solution for our extended data set with no data filters (see Table 1), and results will be discussed in section 5. Although we do not correct MOPITT observations by the known 6% high bias [*Emmons et al.*, 2007], *Heald et al.* [2004] showed that the effect of the correction on the a posteriori solution was minimal. The observation error covariance matrix $\mathbf{S}_\Sigma$ for use in the inversion is dominated by the forward model error with a spatial covariance structure found by *Heald et al.* [2004] to decay over a second-order autoregressive length scale of 150 km. Since this length scale is less than our grid resolution we treat $\mathbf{S}_\Sigma$ as diagonal. Observational errors are derived with the relative residual error (RRE) method of *Palmer et al.* [2003] and are in the range 5–26%, as shown by *Heald et al.* [2004, Figure 4].

[15] Our a priori CO sources, following *Heald et al.* [2004], include monthly Asian anthropogenic emissions (fossil fuel and biofuel combustion) from *Streets et al.* [2003] and daily biomass burning emissions from *Heald et al.* [2003b], based on the climatology of *Duncan et al.* [2003]. Following *Duncan et al.* [2006], we augment these emissions by 19% (anthropogenic) and 16% (biomass burning) to account for rapid oxidation to CO of coemitted nonmethane volatile organic compounds (NMVOCs). Figure 2 shows the a priori emissions for our simulation period (1 February to 10 April 2001), featuring maxima in the biomass burning regions of India and southeastern Asia as well as high values from fuel use in eastern China. Also following *Heald et al.* [2004], we include in the state vector a separate chemical source of CO lumping production from methane and from biogenic NMVOCs including isoprene,

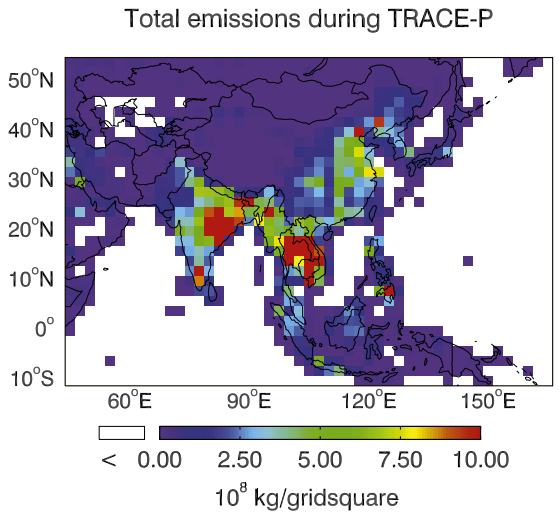

Figure 2. A priori CO source from fossil fuel, biofuel, and biomass burning during the TRACE-P period (1 February to 10 April 2001). The sources are in units of kilograms per 2° × 2.5° grid square.

monoterpenes, acetone, and methanol. This chemical source is as described by *Duncan et al.* [2006].

[16] Following *Heald et al.* [2004], errors on the a priori fuel CO sources are taken from *Streets et al.* [2003] and capped at 100%. Errors on the biomass burning sources are assumed to be 50%, and these two errors are added in quadrature and again capped at 100% to obtain the regional source error, which ranges from 17% in Japan to 100% in southeastern Asia, India, Philippines, and Indonesia. We assume errors to be spatially uncorrelated so that $\mathbf{S_a}$ is diagonal.

4. GEOS-Chem Forward Model and Its Adjoint

[17] The GEOS-Chem CTM used as forward model in the inversion is driven here by assimilated meteorological data from the Goddard Earth Observing System (GEOS-3) of the NASA Global Modeling and Assimilation Office (GMAO). We use a linear CO simulation (GEOS-Chem version 6-02-05; http://www-as.harvard.edu/chemistry/trop/geos) with stored monthly mean OH concentration fields from a previous O_3-NO_x-NMVOC simulation [*Fiore et al.*, 2003]. Our global annual mean pressure-weighted OH concentration below 200 hPa is 1.00×10^6 cm^{-3}. The resolution is $2^\circ \times 2.5^\circ$ in the horizontal, with 30 vertical levels and 15 min transport time steps. We apply local MOPITT averaging kernels [*Deeter et al.*, 2002] to the GEOS-Chem vertical profiles of CO and obtain column values for comparison to MOPITT (Figure 1). The MOPITT averaging kernels have greatest sensitivity in the middle troposphere. Our linear CO simulation is the same as that used in previous applications of GEOS-Chem to interpret CO observations from the TRACE-P period [*Heald et al.*, 2003a; *Jones et al.*, 2003; *Palmer et al.*, 2003; *Heald et al.*, 2004; *Wang et al.*, 2004].

[18] Our forward and adjoint model simulations cover the February–April 2001 period, starting from observed fields on 1 February. This initialization is done by spinning up GEOS-Chem from January 2000 to February 2001 and then adjusting the 1 February 2001, model CO concentrations by the ratio of mean model CO columns in each 2° zonal band to the corresponding MOPITT observations on that day. The adjustment factors range from +20% in the tropics to +4–8% at northern midlatitudes and −2% in the Arctic. Such an adjustment was not done in the work by *Heald et al.* [2004], where instead the inversion optimized for year-round emissions assuming known temporal variability. This would cause some difference with our results if the correction factors for the emissions after 1 February are different from those before, although there is no particular reason why that should be so. The 1 February adjustment in our work also corrects the latitudinal background so that our observational error derived from the RRE method is slightly lower (by up to 3%) than in the work by *Heald et al.* [2004]. We did not implement MOPITT scaling and 1 February start date in order to preserve as much of the analytical inversion setup as possible.

[19] The construction and theoretical validation of the GEOS-Chem adjoint is presented by *Henze et al.* [2007] in the context of an aerosol source inversion. The adjoint code was derived from the forward code using a (discrete) adjoint of algorithms approach [*Giering and Kaminski*, 1998]. The exception was the adjoint of the advection operator, for which the continuous approach was adopted, wherein the adjoint model equations are solved using the same *Lin and Rood* [1996] advection scheme as in the forward model but with reverse winds. Although the advective component of the adjoint leads to sensitivities (gradients) that differ from forward model sensitivities, these discrepancies are not inaccuracies in either discrete or continuous approach, as has been discussed extensively in previous work [e.g., *Sirkes and Tziperman*, 1997; *Thuburn and Haine*, 2001; *Vukicevic et al.*, 2001; *Hakami et al.*, 2007; *Henze et al.*, 2007]. In fact, a continuous approach to an adjoint of advective component has been shown to successfully constrain even a point source [*Davoine and Bocquet*, 2007]. We added here self-adjoint modules for CO emissions and chemical loss (these operator matrices are diagonal and thus are not modified by transposition), as well as the adjoint (transpose) of the MOPITT averaging kernel matrices. The cost function gradient computed by the adjoint model is used with a bounded quasi-Newtonian limited-memory BFGS optimization [*Liu and Nocedal*, 1989] to obtain the MAP solution for CO sources. In addition to testing of the adjoint model conducted and previously reported by *Henze et al.* [2007], we performed a series of Observation System Simulation Experiments (OSSEs), wherein we ascertained the ability of the optimization system to successfully constrain CO sources given a varied density of data.

5. Implementation of the Adjoint Method

[20] Our adjoint solution optimizes the combustion sources of CO (treated as surface fluxes) at the global $2^\circ \times 2.5^\circ$ horizontal resolution of the forward model. The state vector consists of time-invariant correction factors with a zero lower bound imposed by the optimization algorithm, applied to the a priori inventory for the model grid squares where these emissions are nonzero (3013 out of 13,104 surface grid squares). Temporal variability of emissions is assumed to be adequately constrained by the a priori emission inventories of *Streets et al.* [2003] and *Heald et al.* [2003b] (monthly for fuel, daily for biomass burning) and so is not optimized here. We add a correction factor to optimize the background source from oxidation of methane and biogenic NMVOCs, so that the state vector has 3014 elements. The inversion is conducted for the TRACE-P period (1 February to 10 April or 69 days).

[21] We initialized the GEOS-Chem CO field on 1 February with MOPITT observations as described in section 4. As a result, the sensitivity of the cost function to emissions before 1 February is negligibly small; the norm of the corresponding cost function gradient (0.01) is much smaller than the norms of the a priori (7.20) and a posteriori (0.35) cost function gradients. We determined an optimal value $\gamma = 0.01$ for the regularization parameter as that which yields the lowest a posteriori value of the cost function (Figure 3), however all values of γ that are smaller than 1 yield an a posteriori cost function within 1%, essentially eliminating the influence of a priori constraint. When $\gamma > 1$, influence of the a priori limits the optimization of the solution. A likely reason for our need to reduce the weight of the a priori information through γ is that we did not account for spatial correlation of a priori sources, whereas, in fact, CO source

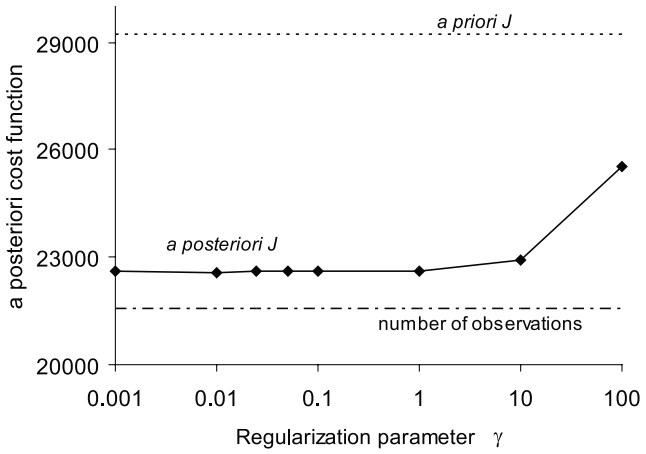

Figure 3. A posteriori cost function $J(\mathbf{x})$ as a function of the regularization parameter γ (equation (2)). The top dotted line is the a priori cost function value, and the bottom dashed line gives the number of MOPITT observations (21,569).

errors within a given geopolitical region are expected to be correlated [*Stavrakou and Müller*, 2006].

[22] With $\gamma = 0.01$, the a posteriori cost function is 22,575 (starting from an a priori value of 29,191). This is comparable to the number of observations used in the inversion (21,569). Figure 4 shows the evolution of the cost function as a function of the iteration number in the inversion. The analytical method using the same data set as the adjoint method has a higher a priori cost function (37,686, see case 3 of Table 1), reflecting the GEOS-Chem initialization in the adjoint method with MOPITT observations on 1 February. The a posteriori cost function from the analytical method (28,762) is higher than from the adjoint method, indicating that the adjoint method provides a better fit to the observations. The a priori source constraint does not contribute significantly to the a posteriori cost function in either the adjoint or the analytical solution.

6. Comparison of Adjoint and Analytical Solutions

[23] Figure 5 shows the a posteriori emission correction factors for the adjoint and analytical solutions. The correction factors for the adjoint solution range from the lower bound of zero (a few grid squares in biomass burning dominated regions in India), to 2.85 (northern China). Average model bias relative to the MOPITT observations decreases from a mean of +2.9% with a priori emissions to −2.0% with a posteriori emissions; however, on a regional scale, the a posteriori model bias is negligible in India, southeastern Asia and southern China, indicating vast improvement. The global source from oxidation of methane and biogenic NMVOCs decreases by only 1%, which provides some confidence in the model concentrations of OH. This confidence justifies in turn focusing the optimization on CO sources, rather than on the sink from oxidation by OH.

[24] The analytical solution in Figure 5 is for case 3 in Table 1, which has exactly the same setup as the adjoint solution. It departs from the best case analytical solution by *Heald et al.* [2004] in that it includes only diagonal terms of the observational error covariance, it uses an expanded data

Figure 4. Cost function $J(\mathbf{x_n})$ for the adjoint solution as a function of iteration number.

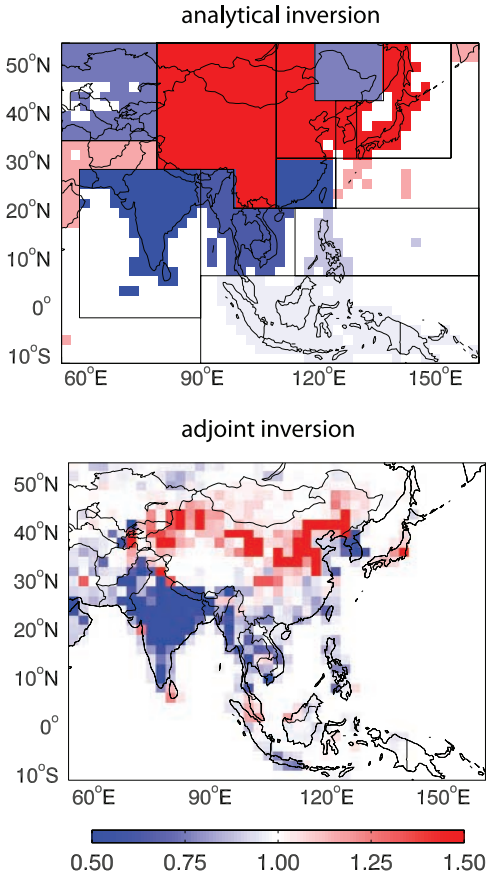

Figure 5. Correction factors to a priori Asian CO sources for February–April 2001 as optimized by (top) the analytical inversion (case 3 of Table 1) and (bottom) the adjoint inversion. Boxes in the top refer to the individual regions (state vector elements) used by *Heald et al.* [2004], as listed in Table 1. The adjoint correction factors are applied individually to all 2° × 2.5° continental grid squares. The color scale saturates at 0.50 and 1.50; correction factors in the adjoint solution range from a lower limit of zero (a few grid squares in biomass burning dominated regions in India), to 2.85 (northern China). The analytical solution is as indicated in Table 1.

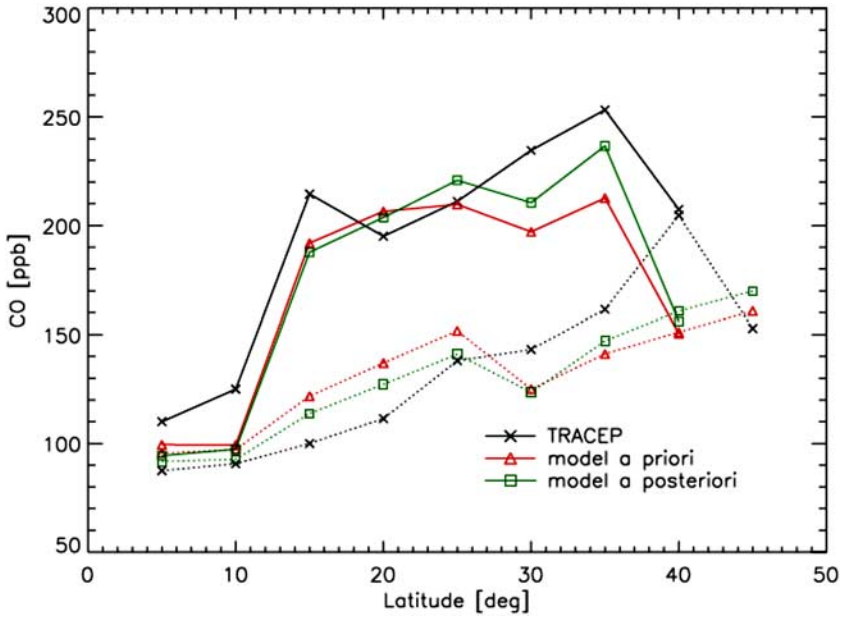

Figure 6. Latitudinal gradient of measured and modeled CO concentrations over TRACE-P domain on a GEOS-Chem 2° × 2.5° grid, averaged over 5° latitude bins. The model CO was sampled along the TRACE-P flight tracks for the flight days and is shown for the simulations with a priori and a posteriori sources in the 0–3 km (solid lines) and >3 km altitude range (dotted lines).

domain, and it does not filter outliers. The effects of these successive changes in the analytical solution relative to the *Heald et al.* [2004] best case are shown as cases 1–3 in Table 1. Also shown in Table 1 are the ranges of results from the ensemble of analytical solutions presented by *Heald et al.* [2004] with varying choices of inversion parameters and MOPITT data processing, representing estimated uncertainty ranges in the inverse analysis. The correction factors obtained from our adjoint solution generally fall well within these ranges but tend to be smaller than for the analytical solution. Error in the adjoint solution would need to be estimated with a similar ensemble approach as in the work by *Heald et al.* [2004], and is likely narrower owing to reduction in the aggregation error.

[25] The fine structure of the adjoint solution is discussed in section 7. Here we compare the adjoint solution averaged over the nine Asian regions of *Heald et al.* [2004] to the corresponding analytical solution for case 3 matching the setup of the adjoint inversion. The analytical solution (case 3 in Table 1) finds large underestimates of emissions in fossil fuel dominated central and western China (by 83% and 138% respectively) and an overestimate in regions with mostly biomass burning emissions (37% in southeastern Asia and 50% in India). The adjoint solution also finds an underestimate of fossil fuel emissions in central and western China (by 34 and 10% respectively) and an overestimate of emissions in southeastern Asia and India (by 22% and 63%, respectively).

[26] A large discrepancy between the two solutions is apparent for Korea and Japan. *Heald et al.* [2004] find an 88% underestimate in Korea-Japan (they were not able to separate constraints on these two regions). The adjoint solution finds only weak corrections with Japan underestimated (11%) but Korea overestimated (6%).

[27] Aircraft observations from the TRACE-P campaign over the NW Pacific in spring 2001 [*Jacob et al.*, 2003] offer an independent evaluation of our adjoint solution. Figure 6 shows the latitudinal gradients of CO concentrations measured by the aircraft in two altitude ranges (0–3 and 3–12 km) and simulated by the model using a priori and a posteriori sources. The observations are averaged over the model grid squares, and the model is sampled at the location and time of the measurements. *Palmer et al.* [2003] previously pointed out that the model with a priori sources overestimates the TRACE-P observations in the free troposphere south of 25°N (excessive biomass burning emissions in SE Asia) and underestimates observations north of 30°N (insufficient Chinese anthropogenic emissions). Our a posteriori solution from the adjoint method affords significant improvement in the simulation of the TRACE-P data, as shown in Figure 6.

7. Fine Structure of the Adjoint Solution and Interpretation

[28] The high-resolution adjoint inversion provides source constraints that distinguish individual cities, for example Tokyo and Mumbai in Figure 5. The adjoint inversion takes advantage of MOPITT's ability to detect urban centers [*Clerbaux et al.*, 2008]. It also distinguishes political boundaries as between China, Korea, and Japan, although these are not implemented as a priori constraints. It reveals compensating patterns of underestimate and overestimate within the same previously aggregated region of the analytical solution. This is most manifested in previously aggregated regions of India and Indonesia. In the Indian region from *Heald et al.* [2004], we find an underestimate of emissions in Mumbai, Sri Lanka and northern India, and an overestimate in the rest of India where

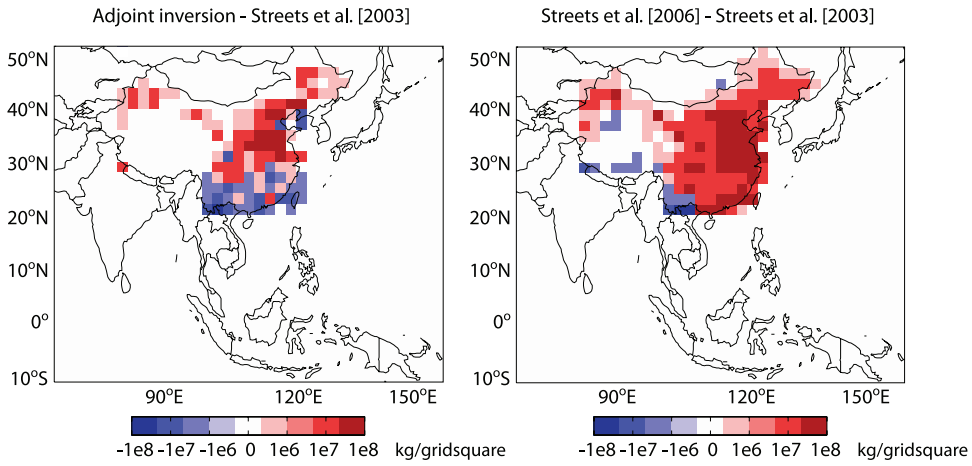

Figure 7. Spatial distribution of the absolute emissions corrections to the *Streets et al.* [2003] CO emission inventory as obtained by the (left) adjoint inversion and by the (right) *Streets et al.* [2006] revised bottom-up inventory. Results are shown on the GEOS-Chem 2° × 2.5° grid for the 1 February to 10 April 2001 period.

biomass burning emissions dominate. In the Indonesia region from *Heald et al.* [2004], emissions from Singapore and northern Indonesia are underestimated, but this is compensated on the regional scale by an overestimate of mostly biofuel emissions from Java (including Jakarta and other major cities. This points to the danger of aggregating large regions to afford analytical solution to the inverse problem.

[29] *Streets et al.* [2006] recently revisited their previous Chinese CO emissions inventory for the TRACE-P period [*Streets et al.*, 2003] in light of evidence from inverse analyses of the TRACE-P and MOPITT data that their anthropogenic emission estimates from China (116 Tg CO a^{-1}) were too low by 40–55% [*Palmer et al.*, 2003; *Heald et al.*, 2004; *Wang et al.*, 2004]. We find the Chinese CO emissions underestimate to be only 15% (Table 1). The updated *Streets et al.* [2006] inventory for China in 2001 is 157 Tg CO a^{-1}, 36% higher than that of *Streets et al.* [2003] due to inclusion of previously neglected sources (e.g., power plants, small coke ovens, synthetic ammonia production, unregistered rural vehicles, and coal mine fires), an update with 2001 data on activity rates, and corrections to emission factors (e.g., cement kilns, iron and steel industries, and vehicles).

[30] Figure 7 compares the geographical distribution of the corrections to the *Streets et al.* [2003] inventory from our adjoint inversion and from the revised bottom-up inventory of *Streets et al.* [2006]. Both show large and consistent upward corrections in central and eastern China. They agree on upward correction in northern China (where the "best estimate" *Heald et al.* [2004] inversion pointed to a downward correction) and in western China. There are however large discrepancies in southern China, where both the adjoint and analytical inversions find the need for downward correction but *Streets et al.* [2006] only find decreases in the southern edge of the country near the Myanmar border (where emissions are mostly from biomass burning). *Streets et al.* [2006] find large upward corrections in coastal southern China that are not seen in the adjoint inversion.

[31] A recent biomass burning inventory for 2001 by *van der Werf et al.* [2006] using MODIS satellite fire counts finds much smaller CO emissions than the *Heald et al.* [2003b] inventory for India and southeastern Asia used here as a priori. They find biomass burning CO emissions to be largely absent in India and about 36% below *Heald et al.* [2003b] in southeastern Asia, which agrees closely with the adjoint solution (Table 1 and Figure 5).

8. Conclusions

[32] We presented a comparison of adjoint and analytical methods for inverting Asian CO sources on the basis of MOPITT satellite observations of CO columns over Asia and the North Pacific during the TRACE-P aircraft campaign (February–April 2001).The adjoint method provides a powerful tool for exploiting high-density observations of atmospheric composition from space to constrain emissions with high resolution. The standard analytical method, requiring construction and operations of the Jacobian matrix of the forward model, is severely limited in terms of the source information that it can resolve. Our motivation was to illustrate the capability of the adjoint method through comparison to the analytical method. Several previous studies had applied the analytical method to invert Asian CO sources on the basis of MOPITT and TRACE-P data for the same period.

[33] We started from the previous analytical inversion by *Heald et al.* [2004] which used MOPITT CO column observations for the TRACE-P period, and the GEOS-Chem chemical transport model (CTM) as forward model, to constrain CO sources from 9 Asian regions. We used the same MOPITT observations, forward model, a priori source information, and error characterization as *Heald et al.* [2004], but optimized the Asian CO sources at the 2° × 2.5° horizontal grid resolution of the CTM rather than for the 9 coarse regions of *Heald et al.* [2004]. The resulting a posteriori cost function is lower in the adjoint solution than in the analytical solution, indicating a better fit to the observations.

[34] We compared the results from the adjoint and analytical inversions by averaging over the 9 coarse Asian regions of the latter. The large-scale features of the a posteriori source constraints are very similar in both solutions; a priori Chinese fossil fuel and biofuel emissions are underestimated in the *Streets et al.* [2003] inventory, and emissions from biomass burning regions in India and southeastern Asia are overestimated in the *Heald et al.* [2003b] inventory. However, correction factors in the adjoint solution tend to be smaller than in the analytical solution. Also, the analytical solution finds the need for large increases in emissions in Korea-Japan, whereas the adjoint solution finds only a small increase in Japan and a decrease in Korea.

[35] The high resolution of the adjoint solution provides constraints on emissions are the scale of individual cities, and reveals particularly large underestimation of CO emissions from Tokyo and Mumbai. The adjoint solution can also resolve geographical boundaries between China, Korea, and Japan even though these are not in the a priori constraints. Comparison of the adjoint and analytical solutions warns of large aggregation errors when optimizing sources averaged over coarse regions in the analytical solution. For example, in the Indian subcontinent, the adjoint solution is able to separate increases in Mumbai, northern India, and Sri Lanka from decreases in the rest of the region where the seasonal source is mostly from biomass burning.

[36] *Streets et al.* [2006] recently revised their prior 2001 anthropogenic emission inventory for China [*Streets et al.*, 2003] to address the underestimates found in previous inverse model analyses. They added previously neglected sources, updated information on activity rates, and corrected emission factors. Their updated inventory finds a 36% increase over the prior, as compared to 41–55% found in previous inverse studies and 15% in our work. Our adjoint solution agrees with *Streets et al.* [2006] in attributing most of the increase to central and eastern China where emissions are highest. However, there are inconsistencies in the fine structure, and *Streets et al.* [2006] find the need for significant upward corrections in southern China that are not apparent in our adjoint or analytical inversions. The recent biomass burning inventory of *van der Werf et al.* [2006] yields estimates for eastern India and southeastern Asia that are much lower than *Heald et al.* [2003b] and consistent with our results. Independent comparison with in situ aircraft CO data from TRACE-P campaign shows improved model-data agreement when a posteriori sources instead of a priori sources are used.

[37] **Acknowledgments.** This work was supported by the NASA Atmospheric Chemistry Modeling and Analysis Program, by the Jet Propulsion Laboratory of the California Institute of Technology under contract with NASA, and by NASA Headquarters under the Earth System Science Fellowship grant NGT5 06-ESSF06-45 to Monika Kopacz. The authors would also like to thank Dylan Jones, Parvadha Suntharalingam, Ronald Errico, and Christopher Holmes for useful insight and discussions.

References

Allen, D., K. Pickering, and M. Fox-Rabinovitz (2004), Evaluation of pollutant outflow and CO sources during TRACE-P using model-calculated, aircraft-based, and Measurements of Pollution in the Troposphere (MOPITT)-derived CO concentrations, *J. Geophys. Res.*, *109*, D15S03, doi:10.1029/2003JD004250.

Arellano, A. F., P. S. Kasibhatla, L. Giglio, G. R. van der Werf, and J. T. Randerson (2004), Top-down estimates of global CO sources using MOPITT measurements, *Geophys. Res. Lett.*, *31*, L01104, doi:10.1029/2003GL018609.

Arellano, A. F., P. S. Kasibhatla, L. Giglio, G. R. van der Werf, J. T. Randerson, and G. J. Collatz (2006), Time-dependent inversion estimates of global biomass-burning CO emissions using Measurement of Pollution in the Troposphere (MOPITT) measurements, *J. Geophys. Res.*, *111*, D09303, doi:10.1029/2005JD006613.

Arellano, A. F., Jr., K. Raeder, J. L. Anderson, P. G. Hess, L. K. Emmons, D. P. Edward, G. G. Pfister, T. L. Campos, and G. W. Sachse (2007), Evaluating model performance of an ensemble-based chemical data assimilation system during INTEX-B field mission, *Atmos. Chem. Phys.*, *7*, 5695–5710.

Baker, D. F., S. C. Doney, and D. S. Schimel (2006), Variational data assimilation for atmospheric CO_2, *Tellus, Ser. B*, *58*, 359–365, doi:10.1111/j.1600-0889.2006.00218.x.

Bergamaschi, P., R. Hein, M. Heimann, and P. J. Crutzen (2000), Inverse modeling of the global CO cycle: 1. Inversion of CO mixing ratios, *J. Geophys. Res.*, *105*(D2), 1909–1927, doi:10.1029/1999JD900818.

Bousquet, P., P. Ciais, P. Peylin, M. Ramonet, and P. Monfray (1999), Inverse modeling of annual atmospheric CO2 sources and sinks: 1. Method and control inversion, *J. Geophys. Res.*, *104*(D21), 26,161–26,178, doi:10.1029/1999JD900342.

Carmichael, G. R., et al. (2003), Evaluating regional emission estimates using the TRACE-P observations, *J. Geophys. Res.*, *108*(D21), 8810, doi:10.1029/2002JD003116.

Clerbaux, C., D. P. Edwards, M. Deeter, L. Emmons, J. F. Lamarque, X. X. Tie, S. T. Massie, and J. Gille (2008), Carbon monoxide pollution from cities and urban areas observed by the Terra/MOPITT mission, *Geophys. Res. Lett.*, *35*, L03817, doi:10.1029/2007GL032300.

Davoine, X., and M. Bocquet (2007), Inverse modelling-based reconstruction of the Chernobyl source term available for long-range transport, *Atmos. Chem. Phys.*, *7*, 1549–1564.

Deeter, M. N., G. L. Francis, D. P. Edwards, J. C. Gille, E. McKerman, and J. R. Drummond (2002), Operational validation of the MOPITT instrument optical filters, *J. Atmos. Oceanic Technol.*, *19*, 1772–1782.

Dubovik, O., T. Lapyonok, Y. J. Kaufman, M. Chin, P. Ginoux, R. A. Kahn, and A. Sinyuk (2008), Retrieving global aerosol sources from satellites using inverse modeling, *Atmos. Chem. Phys.*, *8*, 209–250.

Duncan, B. N., R. V. Martin, A. C. Staudt, R. Yevich, and J. A. Logan (2003), Interannual and seasonal variability of biomass burning emissions constrained by satellite observations, *J. Geophys. Res.*, *108*(D2), 4100, doi:10.1029/2002JD002378.

Duncan, B. N., J. A. Logan, I. Bey, I. A. Megretskaia, R. M. Yantosca, P. C. Novelli, N. B. Jones, and C. P. Rinsland (2006), Global budget of CO, 1988–1997: Source estimates and validation with a global model, *J. Geophys. Res.*, *112*, D22301, doi:10.1029/2007JD008459.

Eibern, H., and H. Schmidt (1999), A four-dimensional variational chemistry data assimilation scheme for Eulerian chemistry transport modeling, *J. Geophys. Res.*, *104*(D15), 18,583–18,598, doi:10.1029/1999JD900280.

Elbern, H., H. Schmidt, and A. Ebel (1997), Variational data assimilation for tropospheric chemistry modeling, *J. Geophys. Res.*, *102*(D13), 15,967–15,985, doi:10.1029/97JD01213.

Emmons, L. K., G. G. Pfister, D. P. Edwards, J. C. Gille, G. Sachse, D. Blake, S. Wofsy, C. Gerbig, D. Matross, and P. Nedelec (2007), Measurements of Pollution in the Troposphere (MOPITT) validation exercises during summer 2004 field campaigns over North America, *J. Geophys. Res.*, *112*, D12S02, doi:10.1029/2006JD007833.

Fiore, A., D. J. Jacob, H. Liu, R. M. Yantosca, T. D. Fairlie, and Q. Li (2003), Variability in surface ozone background over the United States: Implications for air quality policy, *J. Geophys. Res.*, *108*(D24), 4787, doi:10.1029/2003JD003855.

Giering, R., and T. Kaminski (1998), Recipes for adjoint code construction, *Trans. Math. Software*, *24*(4), 437–474, doi:10.1145/293686.293695.

Hakami, A., D. K. Henze, J. H. Seinfeld, T. Chai, Y. Tang, G. R. Carmichael, and A. Sandu (2005), Adjoint inverse modeling of black carbon during the Asian Pacific Regional Aerosol Characterization Experiment, *J. Geophys. Res.*, *110*(D14), D14301, doi:10.1029/2004JD005671.

Hakami, A., D. K. Henze, J. H. Seinfeld, K. Singh, S. Kim, D. Byun, and Q. Li (2007), The adjoint of CMAQ, *Environ. Sci. Technol.*, *41*(22), 7807–7817, doi:10.1021/es070944p.

Heald, C. L., et al. (2003a), Asian outflow and trans-Pacific transport of carbon monoxide and ozone pollution: An integrated satellite, aircraft, and model perspective, *J. Geophys. Res.*, *108*(D24), 4804, doi:10.1029/2003JD003507.

Heald, C. L., D. J. Jacob, P. I. Palmer, M. J. Evans, G. W. Sachse, H. B. Singh, and D. R. Blake (2003b), Biomass burning emission inventory with daily resolution: Application to aircraft observations of Asian outflow, *J. Geophys. Res.*, *108*(D21), 8811, doi:10.1029/2002JD003082.

Heald, C. L., D. J. Jacob, D. B. A. Jones, P. I. Palmer, J. A. Logan, D. G. Streets, G. W. Sachse, J. C. Gille, R. N. Hoffman, and T. Nehrkorn (2004), Comparative inverse analysis of satellite (MOPITT) and aircraft (TRACE-P) observations to estimate Asian sources of carbon monoxide, *J. Geophys. Res.*, *109*, D15S04, doi:10.1029/2004JD005185.

Henze, D. K., A. Hakami, and J. H. Seinfeld (2007), Development of the adjoint of GEOS-Chem, *Atmos. Chem. Phys.*, *7*, 2413–2433.

Jacob, D. J., J. H. Crawford, M. M. Kleb, V. S. Connors, R. J. Bendura, J. L. Raper, G. W. Sachse, J. C. Gille, L. Emmons, and C. L. Heald (2003), Transport and Chemical Evolution over the Pacific (TRACE-P) aircraft mission: Design, execution, and first results, *J. Geophys. Res.*, *108*(D20), 9000, doi:10.1029/2002JD003276.

Jones, D. B. A., K. W. Bowman, P. I. Palmer, J. R. Worden, D. J. Jacob, R. N. Hoffman, I. Bey, and R. M. Yantosca (2003), Potential of observations from the Tropospheric Emission Spectrometer to constrain continental sources of carbon monoxide, *J. Geophys. Res.*, *108*(D24), 4789, doi:10.1029/2003JD003702.

Kaminski, T., M. Heimann, and R. Giering (1999), A coarse grid three-dimensional global inverse model of the atmospheric transport:1. Adjoint model and Jacobian matrix, *J. Geophys. Res.*, *104*(D15), 18,535–18,553, doi:10.1029/1999JD900147.

Kasibhatla, P., A. Arellano, J. A. Logan, P. I. Palmer, and P. Novelli (2002), Top-down estimate of a large source of atmospheric carbon monoxide associated with fuel combustion in Asia, *Geophys. Res. Lett.*, *29*(19), 1900, doi:10.1029/2002GL015581.

Lin, S. J., and R. B. Rood (1996), Multidimensional flux-form semi-Lagrangian transport schemes, *Mon. Weather Rev.*, *124*, 2046–2070, doi:10.1175/1520-0493(1996)124<2046:MFFSLT>2.0.CO;2.

Liu, D. C., and J. Nocedal (1989), On the limited memory BFGS method for large scale optimization, *Math. Program.*, *45*, 503–528, doi:10.1007/BF01589116.

Müller, J. F., and T. Stavrakou (2005), Inversion of CO and NOx emissions using the adjoint of the IMAGES model, *Atmos. Chem. Phys.*, *5*, 1157–1186.

Palmer, P. I., D. J. Jacob, D. B. A. Jones, C. L. Heald, R. M. Yantosca, J. A. Logan, G. W. Sachse, and D. G. Streets (2003), Inverting for emissions of carbon monoxide from Asia using aircraft observations over the western Pacific, *J. Geophys. Res.*, *108*(D21), 8828, doi:10.1029/2003JD003397.

Palmer, P. I., P. Suntharalingam, D. B. A. Jones, D. J. Jacob, D. G. Streets, Q. Y. Fu, S. A. Vay, and G. W. Sachse (2006), Using CO_2: CO correlations to improve inverse analyses of carbon fluxes, *J. Geophys. Res.*, *111*(D12), D12318, doi:10.1029/2005JD006697.

Pétron, G., C. Granier, B. Khattatov, J. F. Lamarque, V. Yudin, J. F. Muller, and J. Gille (2002), Inverse modeling of carbon monoxide surface emissions using Climate Monitoring and Diagnostics Laboratory network observations, *J. Geophys. Res.*, *107*(D24), 4761, doi:10.1029/2001JD001305.

Pétron, G., C. Granier, B. Khattatov, V. Yudin, J. F. Lamarque, L. Emmons, J. Gille, and D. P. Edwards (2004), Monthly CO surface sources inventory based on the 2000–2001 MOPITT satellite data, *Geophys. Res. Lett.*, *31*, L21107, doi:10.1029/2004GL020560.

Peylin, P., D. Baker, J. Sarmiento, P. Ciais, and P. Bousquet (2002), Influence of transport uncertainty on annual mean and seasonal inversions of atmospheric CO_2 data, *J. Geophys. Res.*, *107*(D19), 4385, doi:10.1029/2001JD000857.

Rodgers, C. D. (2000), *Inverse Methods for Atmospheric Sounding*, World Sci., Tokyo.

Sirkes, Z., and E. Tziperman (1997), Finite difference of adjoint or adjoint of finite difference?, *Mon. Weather Rev.*, *125*, 3373–3378, doi:10.1175/1520-0493(1997)125<3373:FDOAOA>2.0.CO;2.

Stavrakou, T., and J. F. Müller (2006), Grid-based versus big region approach for inverting CO emissions using Measurement of Pollution in the Troposphere (MOPITT) data, *J. Geophys. Res.*, *111*, D15304, doi:10.1029/2005JD006896.

Streets, D. G., et al. (2003), An inventory of gaseous and primary aerosol emissions in Asia in the year 2000, *J. Geophys. Res.*, *108*(D21), 8809, doi:10.1029/2002JD003093.

Streets, D. G., Q. Zhang, L. Wang, K. He, J. Hao, Y. Wu, Y. Tang, and G. R. Carmichael (2006), Revisiting China's CO emissions after Transport and Chemical Evolution over the Pacific (TRACE-P): Synthesis of inventories, atmospheric modeling, and observations, *J. Geophys. Res.*, *111*, D14306, doi:10.1029/2006JD007118.

Thuburn, J., and T. W. N. Haine (2001), Adjoints of nonoscillatory advection schemes, *J. Comput. Phys.*, *171*, 616–631, doi:10.1006/jcph.2001.6799.

van der Werf, G. R., J. T. Randerson, L. Giglio, G. J. Collatz, P. S. Kasibhatla, and A. F. Arellano Jr. (2006), Interannual variability in global biomass burning emissions from 1997 to 2004, *Atmos. Chem. Phys.*, *6*, 3423–3441.

Vukicevic, T., M. Steyskal, and M. Hecht (2001), Properties of advection algorithms in the context of variational data assimilation, *Mon. Weather Rev.*, *129*, 1221–1231.

Wang, Y. X. X., M. B. McElroy, T. Wang, and P. I. Palmer (2004), Asian emissions of CO and NOx: Constraints from aircraft and Chinese station data, *J. Geophys. Res.*, *109*, D24304, doi:10.1029/2004JD005250.

Yumimoto, K., and I. Uno (2006), Adjoint inverse modeling of CO emissions over eastern Asia using four-dimensional variational data assimilation, *Atmos. Environ.*, *40*(35), 6836–6845, doi:10.1016/j.atmosenv.2006.05.042.

C. L. Heald, Department of Atmospheric Science, Colorado State University, Fort Collins, CO 80525, USA.

D. K. Henze, Department of Mechanical Engineering, University of Colorado, Boulder, CO 80309, USA.

D. J. Jacob and M. Kopacz, Division of Engineering and Applied Science, Harvard University, 29 Oxford Street, Cambridge, MA 02138, USA. (mak@io.as.harvard.edu)

D. G. Streets and Q. Zhang, Decision and Information Sciences Division, Argonne National Laboratory, 9700 S. Cass Avenue, Argonne, IL 60439, USA.